

1,2,3,5. J.M. ABDUL, 1-4. L.H. CHOWN, 6. Y. L. SHUAIB-BABATA

CORROSION BEHAVIOUR OF Ti-V-Cr-Rh ALLOY ELECTRODE IN 6M KOH

¹ School of Chemical and Metallurgical Engineering,

² African Materials Science and Engineering Network (AMSEN),

³ Materials for Energy Research Group (MERG),

⁴ DST-NRF Centre of Excellence in Strong Materials, University of the Witwatersrand, Johannesburg, SOUTH AFRICA

⁵ Department of Mechanical Engineering, Federal Polytechnic, Offa, NIGERIA

⁶ Department of Materials and Metallurgical Engineering, University of Ilorin, Ilorin, NIGERIA

Abstract: Corrosion behaviour of $Ti_{25-0.5x}V_{40}Cr_{35-0.5x}Rh_x$ ($x = 0, 0.5, 1$ at %) alloy electrode in 6M KOH was investigated. The V-rich alloy was produced under argon atmosphere in an open hearth crucible furnace. The microstructure of the arc-melted alloy was examined by scanning electron microscopy, and the phases were identified by X-ray diffraction. The as-cast alloys contained a primary (V) body centered cubic phase and an intergranular αTi phase. Rhodium (Rh) decreased the E_{corr} from -767 mV to -793 mV for 0.05 Rh and -825 mV for 0.10 Rh. The corrosion current also decreased from $1 \mu A/cm^2$ in Rh-free alloy to $0.77 \mu A/cm^2$ with addition of 0.05 at % Rh and $0.37 \mu A/cm^2$ with addition of 0.10 at.% Rh. Addition of 0.05 at. % Rh decreased the corrosion rate from 0.0110 to 0.0009 mm/y and to 0.001 mm/y with addition of 0.10 at.% Rh. Hardness of the alloy electrode decreased with addition of rhodium.

Keywords: Corrosion Behaviour, V-rich Alloy, 6M KOH, αTi Phase, Body Centre Cubic Phase

INTRODUCTION

Palladium Group Metals, PGM are known for inhibiting corrosion. Schutz (1996) found that corrosion challenges of titanium (Ti)-based alloys in aggressive environments can be practically and cost effectively overcome by minor additions of platinum group metals such as palladium (Pd) and ruthenium (Ru) at < 0.25 at.%. Also, the corrosion rate of titanium metal surfaces exposed to strong acid media was highly inhibited by coating the surface with rhodium (Rh) (Lal *et al.*, 1982); addition of 0.04 - 0.08 wt% Pd to Ti-3Al-2.5V, Ti-6Al-4V, Ti-3Al-5V-6Cr-4Zr-4Mo alloys greatly improved the corrosion resistance in dilute sulphuric acid (Schutz, 1996). Ruthenium additions to Ti-3Al-2.5V, Ti-6Al-4V, Ti-3Al-5V-6Cr-4Zr-4Mo alloys effectively inhibited titanium crevice corrosion in hot halite and sulphate environments (Schutz & Speller, 2003). Corrosion rate of CP-Ti was considerably lowered in 6, 9 and 11.5M HNO_3 , and boiling 15.65M HNO_3 when alloyed with Ni, Pd, Ru and Cr (Ningshen *et al.*, 2015). Binary alloys formed by addition of 10 wt% Ag, Au, Pd, or Pt to Ti has higher corrosion current density (Hwang, *et al.*, 2015). Yamamoto and Kanda (1997) investigated the corrosion behaviour of AB₅ type hydrogen storage alloy in alkaline solution and found that, the effect of heat treatment on corrosion resistance is not significant. This study intends to investigate the corrosion behaviour of rhodium on Ti-V-Cr alloy in 6M KOH solution.

MATERIALS AND METHODS

Melting and casting of the alloy was done in a water-cooled, copper-crucible arc melting furnace under argon atmosphere. In order to ensure homogeneity, the ingot was turned over and remelted three times. The as-cast specimens were cut, mounted, ground and polished to a finish of $0.15 \mu m$ using colloidal silica.

Phase identification was done using optical microscopy and scanning electron microscopy (SEM) with energy dispersive X-ray Spectroscopy (EDX) using an Oxford system. Phases of the alloy were determined by XRD analysis, using the Xpert High Score[®]

phase identification software on a Bruker D2_Phaser[®] X-ray diffraction machine. Analysis was done with Cu-K α radiation from $2\theta = 10^\circ$ to 90° . Further analysis of the alloy was done using a FEI Nova NanoSEM 200[®] scanning electron microscope (SEM) fitted with EDAX[®] advanced microanalysis solution. The approximate amount of the phases was determined by image analysis using ImageJ freeware.

Vickers microhardness tests with a 2 kg load were done on a FutureTech FT FM700[®] machine. The hardness values were measured five times and the average value was recorded.

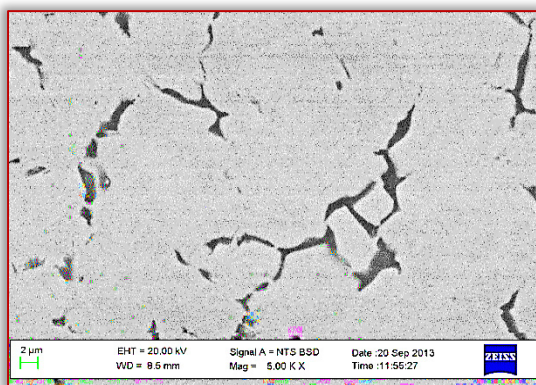
A Potentiodynamic corrosion test was performed using an AutoLab[®] corrosion test apparatus and an electrochemical cell consisting of a tri-electrode: the platinum reference electrode, an Ag/AgCl counter electrode, and the test alloy as the working electrode in 6 M KOH aqueous solution as the electrolyte. The corrosion experiment was performed at 25°C, and a Tafel curve was recorded from -1.4V to -0.2V with a scanning rate of 1 mV/sec.

RESULTS AND DISCUSSION

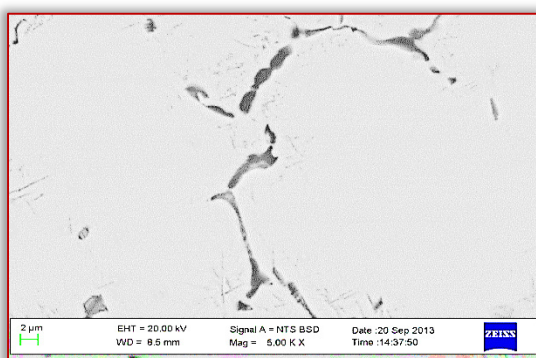
Microstructure of $Ti_{25-0.5x}V_{40}Cr_{35-0.5x}Rh_x$ ($x = 0, 0.5, 1$ at.%) and XRD patterns of as-cast $Ti_{25-0.5x}V_{40}Cr_{35-0.5x}Rh_x$ ($x = 0, 0.05, 0.10$) at.% alloy are respectively presented in Figure 1 and 2.

When 0.05 at.% Rh was substituted for Cr and Ti in $Ti_{25}V_{40}Cr_{35}$, the resulting structure was primary BCC (V) with intergranular Laves phase and a eutectic region surrounding the intergranular Laves regions, as shown in Figure 1. A similar structure was observed with addition of 0.10 at.% Rh but the laves phase was more prominent compared to 0.05 at.% alloy.

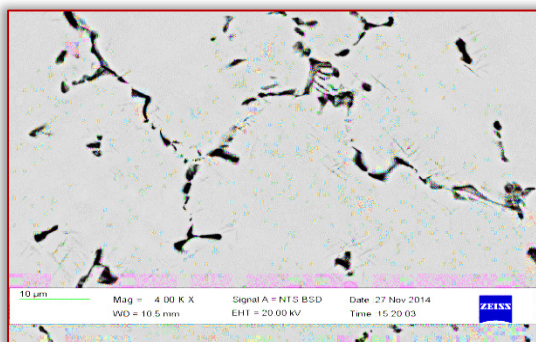
The XRD pattern in Figure 2 shows the main peak of BCC (V) and minor peak of C14 laves corresponding to the dark intergranular αTi phase in the micrograph. EDS of as-cast $Ti_{25-0.5x}V_{40}Cr_{35-0.5x}Rh_x$ ($x = 0, 0.05, 0.10$) is presented in Tables 1-2.



x = 0 at.%



x = 0.05 at.%



x = 1 at.%

Figure 1: Microstructure of $Ti_{25-0.5x}V_{40}Cr_{35-0.5x}Rh_x$ ($x = 0, 0.5, 1$ at.%)

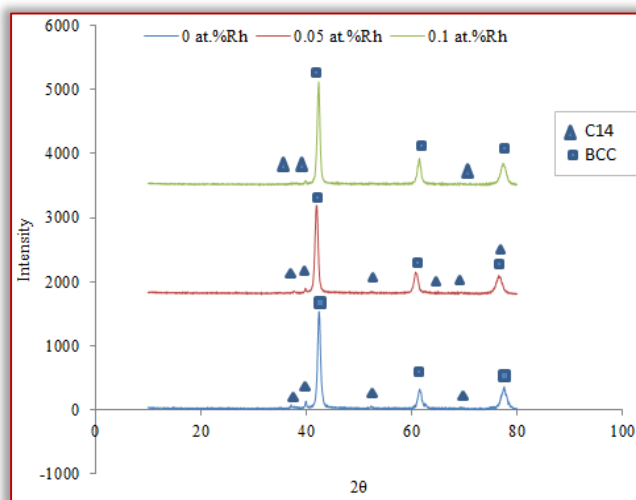


Figure 2: XRD patterns of as-cast $Ti_{25-0.5x}V_{40}Cr_{35-0.5x}Rh_x$ ($x = 0, 0.05, 0.10$) at.% alloy

Table 2 shows that with addition of 0.05 at.% Rh, there was no significant increase in cell volume of Laves and that of BCC. However, in the as-cast 0.10 Rh alloy, the cell volume of BCC increased from 27.67 \AA^3 in Rh-free to 27.75 \AA^3 while that of Laves decreased from 36.24 \AA^3 to 34.48 \AA^3 .

The average of five Vickers hardness values of the as-cast 0, 0.05 and 0.10 at.% Rh samples are 415, 410 and 413 MPa respectively. This implied that the hardness of the as-cast $Ti_{25}V_{40}Cr_{35}$ alloy decreased slightly with Rh addition. The Laves phase has higher hardness than BCC (V) (Basak *et al.*, 2008). Table 1 shows higher proportion of BCC phase and lower proportion of harder Laves phase in the Rh-containing alloys, this could be responsible for the reduction in hardness.

Table 1: EDS of as-cast $Ti_{25-0.5x}V_{40}Cr_{35-0.5x}Rh_x$ ($x = 0, 0.05, 0.10$)

Sample	Phases XRD	Compositions* (at.%)			
		Ti	V	Cr	Rh
0 at.% Rh	BCC (V)	22.0 (0.7)	42.8 (0.46)	35.2 (0.82)	
	αTi	66.1 (1.6)	18.9 (1.2)	15.0 (0.8)	
0.05 at.% Rh	BCC (V)	28.5 (3.8)	38.8 (2.2)	32.7 (1.7)	
	αTi	71.8 (5.8)	14.6 (3.0)	13.5 (2.8)	0.5 (0.4)
0.10 at.% Rh	BCC (V)	20.10 (2.8)	42.4 (3.2)	37.5 (6.1)	
	αTi	62.3 (6.3)	19.1 (3.4)	18.6 (3.2)	0.5 (0.4)

*Standard deviation in parentheses

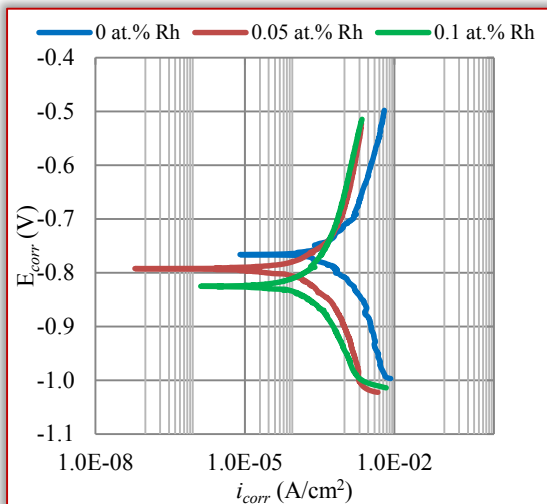
Table 2: EDS of as-cast $Ti_{25-0.5x}V_{40}Cr_{35-0.5x}Rh_x$ ($x = 0, 0.05, 0.10$)

Sample	Vickers hardness (MPa)	Phase proportion (% area)	Space group (No.)	Phase description		Cell vol. (\AA^3)
				A	C	
0 at.% Rh	415	82.5	Im3m (229)	3.0246		27.67
		17.5	P63/mmc (194)	2.98	4.72	36.24
0.05 at.% Rh	410	88.7	Im3m (229)	3.0257		27.70
		11.3	P63/mmc (194)	2.98	4.73	36.25
0.10 at.% Rh	413	83.0	Im3m (229)	3.0275		27.75
		17.0	P63/mmc (194)	2.95	4.67	34.48

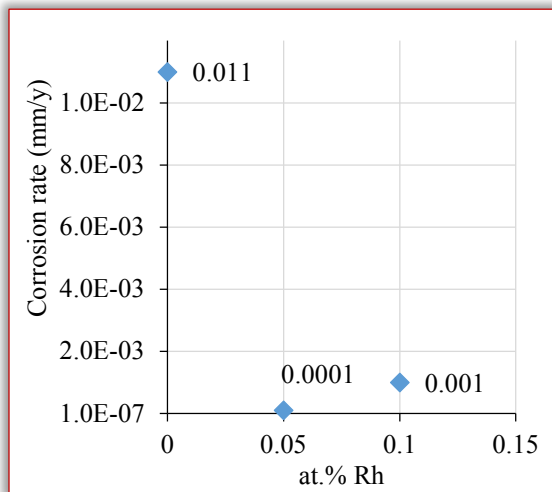
The Tafel's curve and the corresponding corrosion rate for the as-cast $Ti_{25-0.5x}V_{40}Cr_{35-0.5x}Rh_x$ ($x = 0, 0.05, 0.10$) at.% alloy is shown in Figure 3.

Figure 3(a) shows that addition of Rh decreased E_{corr} from -767 mV in Rh-free alloy to -793 mV in 0.05 Rh and -825 mV in 0.10 Rh. The corrosion current also decreased with increase in Rh: from $1 \mu\text{A}/\text{cm}^2$ in Rh-free alloy to $0.77 \mu\text{A}/\text{cm}^2$ with addition of 0.05 Rh, it further decreased to $0.37 \mu\text{A}/\text{cm}^2$ with addition of 0.10 Rh alloy.

In Figure 3(b), addition of 0.05 Rh decreased the corrosion rate from 0.0110 to 0.0009 mm/y but only to 0.001 mm/y with addition of 0.10 Rh. Rhodium is one of the noble metals known as good corrosion inhibitors, so the observed reduction in corrosion rate with addition of Rh agrees with literature. The observed decrease in corrosion rate can be explained by substituting lower electronegativity elements Ti (1.54 Pauling scale) and Cr (1.66) with the higher electronegativity Rh (2.28); since high electronegativity favours a reduction in corrosion rate (Abrashev, *et al.*, 2010). For all the three alloy conditions, the lowest corrosion rate was found with addition of 0.05 Rh, followed by a slight increase in the rate with addition of 0.10 Rh.



(a)



(b)

Figure 3: (a) Potentiodynamic curve (b) corrosion rate of as-cast $Ti_{25-0.5x}V_{40}Cr_{35-0.5x}Rh_x$ ($x = 0, 0.05, 0.10$) at.% alloy

CONCLUSIONS

The following conclusions were drawn from the results of hardness and corrosion rate of $Ti_{25-0.5x}V_{40}Cr_{35-0.5x}Rh_x$ ($x = 0, 0.05, 0.10$) at.% alloys being investigated:

- All the $Ti_{25-0.5x}V_{40}Cr_{35-0.5x}Rh_x$ ($x = 0, 0.05, 0.10$) at.% alloys have BCC (V) as the primary phase and αTi as the intergranular secondary phase.

- Rhodium, Rh decreased the E_{corr} from -767 mV to -793 mV for 0.05 Rh and -825 mV for 0.10 Rh. The corrosion current also decreased from $1 \mu A/cm^2$ in Rh-free alloy to $0.77 \mu A/cm^2$ with addition of 0.05 at.% Rh and $0.37 \mu A/cm^2$ with addition of 0.10 at.% Rh. Addition of 0.05 at.% Rh decreased the corrosion rate from 0.0110 to 0.0009 mm/y and to 0.001 mm/y with addition of 0.10 at.% Rh.
- Hardness of the alloy electrode decreased with addition of rhodium.
- Like other PGM, rhodium inhibits corrosion rate of $Ti_{25}V_{40}Cr_{35}$ alloy, addition of 0.05 at.% Rh is sufficient to reduce the corrosion rate, further addition of Rh is uneconomical since it does not substantially decrease the corrosion rate further.

References

- [1] Abrashev, B., Spassov T, Bliznakov S, & Popov, A: Microstructure and electrochemical hydriding/dehydriding properties of ball-milled TiFe-based alloys. International Journal of Hydrogen Energy, 35(12), 6332-6337, 2010.
- [2] Basak, S; Shashikala, K; & Kulshreshtha, S. K.: Hydrogen absorption characteristics of Zr substituted alloy. International Journal of Hydrogen Energy, 33(1), 350-355, 2008.
- [3] Hwang, M. J.; Park, E.; Moon, W.; Song, H. & Park, Y.: Characterization of passive layers formed on Ti-10 wt% (Ag, Au, Pd, or Pt) binary alloys and their effects on galvanic corrosion.. Corrosion Science, 96, 152-159, 2015.
- [4] Lal, S.; Glen Rock, N. J.; Porcelli, R. W. & Yonkers, N. Y.: Process for inhibiting titanium corrosion, United States Patent, Atlantic Richfield Company, Los Angeles, Calif, (1982), Retrieved from <http://www.patentimages.storage.googleapis.com/pdfs/US4330376.pdf>, on June 16, 2018.
- [5] Ningshen S, Sakairi M, Suzuki K, & Okuno T.: Corrosion performance and surface analysis of Ti-Ni-Pd-Ru-Cr alloy in nitric acid solution. Corrosion Science, 91, 120-128, 2015.
- [6] Schutz, R. W.: Ruthenium enhanced titanium alloys, Platinum Metals Rev., 40(2), 54-61, 1996.
- [7] Schutz, R W. & Speller, F.N.: Award Lecture: Platinum group metal additions to titanium: A highly effective strategy for enhancing corrosion resistance, Corrosion 59(12), 1043-1057, 2003.
- [8] Yamamoto, M. & Kanda M.: Investigation of AB₅ type hydrogen storage alloy corrosion behavior in alkaline electrolyte solutions. Journal of Alloys and Compounds, 253–254, 660-664, 1997.



ISSN: 2067-3809

copyright © University POLITEHNICA Timisoara,
Faculty of Engineering Hunedoara,
5, Revolutiei, 331128, Hunedoara, ROMANIA
<http://acta.fih.upt.ro>